Table II
Yields of Sulfide Products in the Radiolysis of Sulfonium Salts[a]

salt	product (rel yield, %)	conv, %	G^b
Bz_2PhSPF_6	PhBzS	76	8.3
$PhBzMeSPF_6$	PhMeS (97), PhBzS (3)	44	4.8
Ph_2BuSPF_6	Ph_2S (63), PhBuS (37)	41	4.5
Ph_2MeSPF_6	Ph_2S	61	6.6
Bu_2BzSPF_6	Bu_2S (97), BzBuS (3)	18	1.9
Bz_2MeSPF_6	BzMeS (91), Bz_2S (9)	17	1.9

[a] The THF solutions of 1×10^{-2} mol dm^{-3} salts were irradiated for 2 h at a dose rate of 5×10^3 Gy h^{-1} at 0 °C. [b] Number of molecules of a product for a 100-eV energy absorbed by the medium.

The photosensitized polymerization was carried out with solutions containing 1×10^{-3} mol dm^{-3} anthracene as a sensitizer. The solutions were irradiated at wavelengths above 350 nm, where the salts have no absorption. The highly effective initiators for the photosensitized polymerization are Ph_3SPF_6, Bz_2PhSPF_6, and $PhBzMeSPF_6$, similar to the case of direct photoexcitation. On the other hand, Bu_2PhSPF_6, Bz_2MeSPF_6, and Bu_2BzSPF_6 are ineffective, whereas they initiate polymerization by direct photoexcitation. This result should be explained in terms of the sensitization efficiencies for the salts.

When the solutions of the salts were irradiated with γ-rays, the polymerization of THF was initiated with the salts having Ph substituents. As previously reported for Ph_3SPF_6, the salts decompose through one-electron reduction by the solvated electron:[2]

$$Ph_3SPF_6 + e_s^- \rightarrow Ph_2S + Ph^\bullet + PF_6^- \tag{2}$$

The electron scavenging by the salts results in prevention of neutralization of the radiolytically produced cation, THF(H^+), which initiates the polymerization. This is confirmed by the pulse radiolysis experiments similar to the case of Ph_3SPF_6.[2] Pulse radiolysis of THF solutions of an aromatic compound results in the formation of the radical anion of the solute via the attachment of the solvated electron. The effect of the salts on the yield of the radical anion was examined by using *trans*-stilbene as the aromatic solute. The yield of the *trans*-stilbene radical anion was extremely decreased by the addition of the salts, suggesting the occurrence of the competitive electron scavenging by the salts. The yields of the radiation-induced polymerization are in the range from 3.0% to 9.5%. The range is narrow compared with that of the photoinduced polymerization. This may be attributed to the fact that the salts react with the solvated electron, a strongly reducing species, and the reaction is less selective. The results of the pulse radiolysis experiments demonstrated that Bz_2MeSPF_6, Bu_2BzSPF_6, and Bu_3SPF_6 also scavenge the solvated electron, whereas they did not initiate the polymerization. At the present time, no explanation is given for the ineffectiveness of these salts in the radiation-induced polymerization.

The product analysis data for the radiolysis of some sulfonium salts are presented in Table II. The relative yields of the sulfide products demonstrate the leaving group propensity of Bz > methyl ≃ butyl > phenyl. The decomposition yields for Bu_2BzSPF_6 and Bu_2MeSPF_6, not initiating the polymerization, are small compared with those for the other salts. The G values for the salts initiating the polymerization are higher than that for Ph_3SPF_6, which was 1.8 for the 2-h irradiation, in spite of the high polymer yield for Ph_3SPF_6. The high G values suggest the contribution of decomposition processes other than the one-electron reduction by the solvated electron. A radical-initiated decomposition might occur for these sulfonium salts as well as the one-electron reduction. The yields of the photoinduced and radiation-induced polymerization by Ph_2IPF_6 are much larger than those by the sulfonium salts. This has been attributed to the decomposition of Ph_2IPF_6 by a chain reaction initiated by the radical derived from THF.[2,6]

As described above, the reaction of the salts in the radiation-induced polymerization differs from that in the photopolymerization. When irradiated with γ-rays, the salts act as an electron scavenger, whereas they decompose via the excited states upon irradiation with UV light. The difference in the initiation mechanism was evidenced by the effect of the added chlorinated compounds which scavenge electron to give the nucleophilic chloride anion. The radiation-induced polymerization by Ph_3SPF_6 was inhibited by the addition of 10 vol % dichloromethane or carbon tetrachloride, whereas the photopolymerization was not affected by the additives. On the other hand, there was no difference in molecular weight between the polymers produced by the photoinduced and radiation-induced polymerizations, when compared at the same post-polymerization time. The result of the GPC measurements agrees with the fact that living polymerization occurs in both systems.

Acknowledgment. We are grateful to the members of the Radiation Laboratory of this institute for help with the γ-irradiation and pulse radiolysis experiments. We are also indebted to the members of the Material Analysis Center of this institute for the elemental analysis of the prepared sulfonium salts.

Registry No. THF (homopolymer), 24979-97-3; THF (SRU), 25190-06-1; Ph_3SPF_6, 57835-99-1; Bz_2PhSPF_6, 119071-32-8; $PhBzMeSPF_6$, 112406-12-9; Ph_2MeSPF_6, 23686-31-9; Ph_2BuSPF_6, 116737-91-8; Bu_2PhSPF_6, 119108-51-9; Bu_2BzSPF_6, 119071-33-9; Bz_2MeSPF_6, 119071-34-0.

References and Notes

(1) For a review, see: Crivello, J. V. *Adv. Polym. Sci.* **1984**, *62*, 1-48.

(2) Ma, X.-H.; Yamamoto, Y.; Hayashi, K. *Macromolecules* **1987**, *20*, 2703-2706.

(3) Beak, P.; Sullivan, T. A. *J. Am. Chem. Soc.* **1982**, *104*, 4450-4457.

(4) Saeva, F. D.; Morgan, B. P. *J. Am. Chem. Soc.* **1984**, *106*, 4121-4125.

(5) Yamashita, Y.; Kozawa, S.; Hirota, M.; Chiba, K.; Matsui, H.; Hirota, A.; Kodama, M.; Ito, K. *Makromol. Chem.* **1971**, *142*, 171-181.

(6) For radical-initiated chain reactions of iodonium salts, see: (a) Beringer, F. M.; Gindler, E. M.; Rapoport, M.; Taylor, R. J. *J. Am. Chem. Soc.* **1959**, *81*, 351-361. (b) Knapczyk, J. W.; Lubinkowski, J. J.; McEwen, W. E. *Tetrahedron Lett.* **1972**, *35*, 3739-3742. (c) Pappas, S. P.; Gatechair, L. R.; Jilek, J. H. *J. Polym. Sci., Polym. Chem. Ed.* **1984**, *22*, 77-84. (d) Ma, X.-H.; Yamamoto, Y.; Hayashi, K. *J. Org. Chem.* **1988**, *53*, 5443-5445.

Self-Consistent Approximation to Fluorescence Decay in Macromolecules with Energy Migration and Dissociating Traps

KRZYSZTOF SIENICKI[†,‡] and WAYNE L. MATTICE[*,†]

Institute of Polymer Science, The University of Akron, Akron, Ohio 44325, and Institute of Applied Physics, Technical University of Gdansk, 80-952 Gdansk, Poland.

Received September 22, 1988;
Revised Manuscript Received December 13, 1988

1. Introduction

The phenomenon of excitation transport and trapping in fluid and solid solutions of polymers that contain aro-

---

[†] The University of Akron.

[‡] Technical University of Gdansk.

matic rings is a subject of active experimental and theoretical work.[1] From a photophysical point of view, there are two important topological factors that distinguish dilute solid or liquid solutions of macromolecules from solutions of small molecules that contain the same concentration of chromophoric groups. First, the chromophoric groups bonded to a macromolecule do not form a random set but instead have spatial correlations that are determined by the conformational statistics of the real chain. The spatial correlations may be extracted from the conformational partition function expressed in the rotational isomeric-state approximation, as reviewed by Flory.[2] Second, with the exception of infinite networks, a macromolecule is a spatially finite object, and a limited number of chromophores can be sampled by the excitation energy in intramolecular excitation transport.

Realistic conformations of a macromolecule have recently been taken into account in a Monte Carlo simulation of energy migration and trapping in polystyrene.[3] Polymer structure is also incorporated in studies of Fredrickson, Andersen, and Frank (FAF)[4] and Fayer et al.[5] FAF have analyzed excitation migration and transfer in macromolecular chains that contain small concentrations of donors and traps randomly distributed along the chain, using theoretical methods developed for excitation migration and transfer in solutions of small molecules. It has been assumed that spatial correlations exist only between chromophores on the same chain; spatial correlations between chromophores on different chains are absent. In addition, it has been assumed that population of the trap is an irreversible process.

The theoretical model developed by FAF can be extended to treat a macromolecule that contains a different type of trap. This system can be modeled as a polymer that contains a small concentration of a particular kind of label (donor), where pairs of labels have the ability to form intramolecular excimers. The excimers represent the trap in this system. It is assumed that the residence time of the excitation on a particular chromophore is much smaller than the time required for conversion of a nonexcimer-forming site into an excimer-forming site by chain dynamics.[3] Contrary to the system treated by FAF, which contains chemically different donors and traps, the excimer traps formed under ordinary conditions are capable of undergoing dissociation, thereby making population of the trap a reversible process. Dissociation of the trap was not included in the original FAF model. The objective of the present article is the extension of the FAF formalism to the case where dissociation causes population of the trap to be reversible. The concentration of preformed excimers is assumed to be small.[3]

2. Theoretical Model

A. Foundation of the FAF Treatment. FAF have proposed a theoretical model of incoherent transport and trapping of electronic excitations among chromophores on polymer chains on the basis of diagrammatic expressions and self-consistent approximations for infinite-order partial sums developed by GAF[6] and LAF.[7] The solution of the Pauli equation that describes excitation migration and transfer can be expressed as a sum of Green functions:[7]

$$G(\mathbf{r},t) = G^{\mathrm{S}}(t)\,\delta(\mathbf{r}) + G^{\mathrm{M}}(\mathbf{r},t) + G^{\mathrm{T}}(\mathbf{r},t) \tag{2.1}$$

where $G^{\mathrm{S}}(t)$ is the probability that an excitation created at zero time is at time t on the donor chromophore where it originated, and $G^{\mathrm{M}}(\mathbf{r},t)$ and $G^{\mathrm{T}}(\mathbf{r},t)$ are the probabilities that at time t the excitation is on another donor chromophore or trap, respectively, at $\mathbf{r}$ from the site of origin. It is useful to define a function $G^{\mathrm{D}}(t)$ as

$$G^{\mathrm{D}}(t) = G^{\mathrm{S}}(t) + G^{\mathrm{M}}(t) \tag{2.2}$$

where $G^{\mathrm{D}}(t)$ is the probability that an excitation is on a donor at a time t after excitation. The function $G^{\mathrm{M}}(t)$ is defined by

$$G^{\mathrm{M}}(t) = \int \mathrm{d}\mathbf{r}\; G^{\mathrm{M}}(\mathbf{r},t) \tag{2.3}$$

Assuming that energy is transferred with rate constants given by Förster[8] and using the spatial correlation functions for Gaussian chain statistics, FAF derived three-particle approximations for Laplace transformations (denoted by ˆ) of $G^{\mathrm{D}}(t)$ in the form

$$\hat{G}^{\mathrm{D}}(\epsilon) = \epsilon^{-1}\{1 + 2.309\bar{c}_{\mathrm{T}}(\epsilon\tau)^{-1/3} + 1.571c_{\mathrm{T}}(\epsilon\tau)^{-1/2} + ...\} + \{1.397c_{\mathrm{T}}^{2} + \alpha_4(\kappa)\bar{c}_{\mathrm{T}}\bar{c}_{\mathrm{D}}\}(\epsilon\tau)^{-2/3} + \{1.375\bar{c}_{\mathrm{T}}c_{\mathrm{T}} + \alpha_6(\kappa)\bar{c}_{\mathrm{T}}c_{\mathrm{D}}(\epsilon\tau)^{-5/6} + \{0.8966c_{\mathrm{T}}^{2} + \alpha_5(\kappa)c_{\mathrm{T}}c_{\mathrm{D}}(\epsilon\tau)^{-1}\}^{-1} \tag{2.4}$$

The quantities $\alpha_1(\kappa)$, $\alpha_2(\kappa)$, ..., $\alpha_6(\kappa)$ are numerical integrals that depend on the ratio of the Förster radii and are tabulated in Table I of ref 4. Dimensionless intramolecular chromophore concentrations are defined by[7]

$$\bar{c}_{\mathrm{D}} = \pi q_{\mathrm{D}}(R_0^{\mathrm{DD}}/a)^2 \tag{2.5}$$

$$\bar{c}_{\mathrm{T}} = \pi q_{\mathrm{T}}(R_0^{\mathrm{DT}}/a)^2 \tag{2.6}$$

and the dimensionless bulk chromophore concentrations are defined as[7]

$$c_{\mathrm{D}} = (4\pi/3)(R_0^{\mathrm{DD}})^3\rho_{\mathrm{D}} \tag{2.7}$$

$$c_{\mathrm{T}} = (4\pi/3)(R_0^{\mathrm{DT}})^3\rho_{\mathrm{T}} \tag{2.8}$$

The parameters q_{D} and q_{T} represent the average number of donors and traps per segment, a is an effective statistical segment length, and R_0^{DD} and R_0^{DT} represent critical radii for energy migration and trapping, respectively.

B. Inclusion of Trap Dissociation. Recently monomer–excimer (donor–trap) kinetics has been analyzed in terms of rate coefficients.[9] The equations obtained for monomer and excimer fluorescence decays, denoted by $M(t)$ and $E(t)$, respectively, have the form[9]

$$M(t) = \mathcal{L}^{-1}\{M^{(1)}(\epsilon)/(1-\beta)\} \tag{2.9}$$

$$E(t) = \mathcal{L}^{-1}\{E^{(1)}(\epsilon)/(1-\beta)\} \tag{2.10}$$

$$M^{(1)}(t) = \mathcal{L}[I(t) \otimes f_{\mathrm{M}}] \tag{2.11}$$

$$E^{(1)}(t) = \mathcal{L}[I(t) \otimes k(t) \otimes f_{\mathrm{E}}] \tag{2.12}$$

$$f_{\mathrm{E}} = \exp[-(k_{\mathrm{E}} + k_{-1})t] \tag{2.13}$$

$$\beta = \mathcal{L}[k(t)f_{\mathrm{M}} \otimes k_{-1}f_{\mathrm{E}}] \tag{2.14}$$

where $\otimes$ denotes the convolution integral, and $\mathcal{L}$ and $\mathcal{L}^{-1}$ denote the Laplace and the reverse Laplace transformation, respectively. Additionally, $I(t)$ denotes the excitation rate coefficient, k_{E} and k_{-1} are rate constants for excimer fluorescence and excimer dissociation, $k(t)$ is the rate coefficient for excimer formation, and f_{M} is the probability that excitation remains in the donor ensemble at time t after excitation.

In the following part of the paper we will use notation commonly accepted in studies of monomer–excimer phenomena. Thus, FAF donor is monomer (M) and trap is excimer (E). The function $G^{\mathrm{D}}(\epsilon)$ is equivalent to f_{M} (eq 2.11), and the donor and trap (excimer) are indistinguishable from the spectroscopic point of view. Thus the

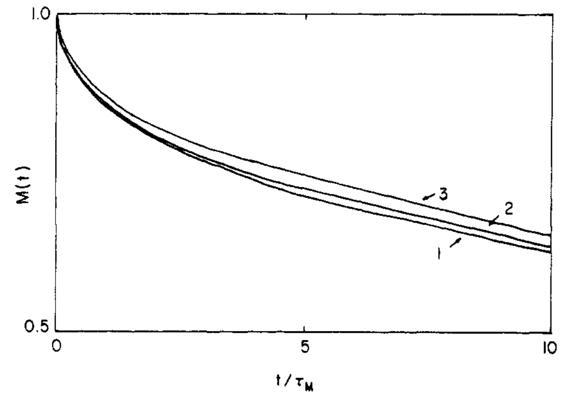

Figure 1. Monomer fluorescence decay $M(t)$ for different values of the dissociation rate constant (k_{-1}). Values of k_{-1} for curves 1–3 in legend 1 - $k_{-1} = 0$, 2 - $k_{-1} = 1.0 \times 10^7$ s^{-1}, and 3 - $k_{-1} = 1.0 \times 10^8$ s^{-1}. In calculations we have used the following parameters: $\tau_M = 1.0 \times 10^{-7}$ s, $k_E = 2 \times 10^7$ s^{-1}.

critical radii in eq 2.5 and 2.6 are the same. We will denote them by R_0. Only one parameter, the rate coefficient $k(t)$ appearing in eq 2.9–2.10, via eq 2.12 and 2.14, must be calculated. The rate coefficient can be defined by

$$k(t) = -\mathrm{d} \ln G^D(t)/\mathrm{d}t \qquad (2.15)$$

so that the excited monomer population obeys the equation

$$\mathrm{d}M_0(t)/\mathrm{d}t = -\tau_M^{-1}M_0(t) - k(t)\, M_0(t) \qquad (2.16)$$

The equivalent equation for the excimer population has the form

$$\mathrm{d}E_0(t)/\mathrm{d}t = -\tau_E^{-1}E_0(t) + k(t)\, M_0(t) \qquad (2.17)$$

It should be emphasized in eq 2.16 and 2.17 that the process of excimer dissociation is not included. If the rate coefficient is of the form specified by eq 2.15, the monomer and excimer fluorescence decays have the forms

$$M(t) = \mathcal{L}^{-1}\{[I(t) \otimes G^D(t)]/ [1 - \mathcal{L}[-G^D(t)\ \mathrm{d} \ln G^D(t)/\mathrm{d}t]\mathcal{L}(k_{-1}f_E)]\} \qquad (2.18)$$

$$E(t) = \mathcal{L}^{-1}\{[I(t) \otimes [-\mathrm{d} \ln G^D(t)/\mathrm{d}t] \otimes G_D(t)]\}/ \{1 - \mathcal{L}[-G^D(t)\ \mathrm{d} \ln G^D(t)/\mathrm{d}t]\mathcal{L}(k_{-1}f_E)\} \qquad (2.19)$$

Equations 2.18 and 2.19 describe monomer and excimer fluorescence decay, respectively, in the presence of energy migration along the chain and reversible trapping by excimers which can dissociate with rate constant k_{-1}.

3. Numerical Analysis

Numerical analysis of the monomer fluorescence has been performed in two steps. With an assumed set of parameters, the function $G_D(t)$ has been calculated over a broad range of t/τ_M by using the Stehfest[10] algorithm. The values of ln $G^D(t)$ have been approximated by a polynomial. The expression obtained in this manner has been recalculated analytically by differentiation with respect to t. Finally, the Laplace transformation, as is required in eq 2.18, has been calculated analytically from the polynomials for $G^D(t)$ and d ln $G^D(t)/\mathrm{d}t$. The Stehfest algorithm was used again in the calculations of the second-step inverse Laplace transformation. It has been assumed that the excitation pulse is in the form of a δ distribution, so that

$$\mathcal{L}[I(t) \otimes G^D(t)] \equiv \mathcal{L}[G^D(t)] \qquad (3.1)$$

Figure 1 depicts the calculated behavior of the monomer fluorescence decay for different values of the dissociate rate constant (k_{-1}) and for $c_D = 1.0$, $\bar{c}_D = 0.01$, $c_T = 0.04$, $\bar{c}_T = 0.0004$, and $\kappa = 1$. The assumption that $\kappa = R_0^{DT}/R_0^{DD} = R_0 \equiv 1$ causes the excimers (traps) to be spectroscopically indistinguishable. An increase in the dissociation rate constant leads to a slower monomer decay. Although the differences in the calculated curves are not dramatic, they are large enough so that the influence of k_{-1} on the decay could be detected by appropriate experiments and analysis.

4. Discussion

The theoretical model used here is based on several assumptions, some of which deserve further comment. It has been assumed that all polymer chains contain at least one site that can form a trap (excimer). The validity of this assumption deteriorates as the degree of polymerization, x, and excimer concentration, q, decrease. Neglecting any influence of polymer dynamics, the probability, p, that a chain cannot form an excimer is approximated as

$$\ln p = (x - 1) \ln (1 - q) \qquad (4.1)$$

If $p > 0$, some excitations cannot be trapped and the total monomer fluorescence decay should be expressed as

$$M_{\mathrm{tot}}(t) = (1 - q)^{x-1} \exp(-t/\tau_M) + [1 - (1 - q)^{x-1}]M(t) \qquad (4.2)$$

where $M(t)$ is given by eq 2.18. If $q > 0$ and $x \rightarrow \infty$, eq 4.2 reduces to eq 2.18.

A second assumption is not explicit in the illustrative calculations presented here. In common with the usual treatment of monomer–excimer kinetics of small aromatic molecules in dilute solution, it has been assumed that dissociation of an excimer necessarily leads to a very large separation of the two chromophores. In some situations, this assumption is not completely correct. Dissociation of an excimer may lead to a transient situation in which the two chromophores remain in close proximity to one another. A local conformational change in the chain molecule may bring the two chromophores back into contact with the orientation required for renewed formation of an excimer. In this situation, the initial formation of the excimer may be controlled by energy migration to an appropriate site, while subsequent repopulation of this site after dissociation is controlled by the rate of local conformational change in the chain. In this system the monomer decay will be of the form

$$M(t) = \mathcal{L}^{-1}\{G^D(\epsilon)(1 + \hat{\beta}) + \widehat{f_0\beta_0}/(1 - \widehat{\beta_0})\} \qquad (4.3)$$

where

$$f_0 = \exp[-(k_E + k_C)t]$$

$$\beta_0 = k_C f_0 \otimes k_{-1} f_E$$

and k_C is the rate constant for excimer formation due to local conformational change in the polymer. It is clear that eq 4.3 differs substantially from eq 2.18.

Acknowledgment. This research was supported by National Science Foundation research grant DMR 86-96071. K.S. expresses appreciation for financial support from Research Project CPBP 01.19.

References and Notes

(1) *Photophysics of Polymers*; Hoyle, C. H., Torkelson, J. M., Eds.; American Chemical Society: Washington, DC, 1987.
(2) Flory, P. J. *Macromolecules* **1974**, *7*, 381.
(3) Blonski, S.; Sienicki, K. *Macromolecules* **1986**, *19*, 2936.
(4) Fredrickson, G. H.; Andersen, H. C.; Frank, C. W. *Macromolecules* **1984**, *17*, 54.

Macromolecules **1989**, *22*, 2857-2858

(5) Ediger, M. D.; Fayer, M. D. *Macromolecules* **1983**, *16*, 1839. Peterson, K. A.; Fayer, M. D. *J. Chem. Phys.* **1986**, *85*, 4702.
(6) Gochanour, C. R.; Andersen, H. C.; Fayer, M. D. *J. Chem. Phys.* **1979**, *70*, 4254.
(7) Loring, R. F.; Andersen, H. C.; Fayer, M. D. *J. Chem. Phys.* **1982**, *76*, 2015.
(8) Förster, Th. *Z. Naturforsch., A: Astrophys., Phys. Phys. Chem.* **1949**, *4A*, 321.
(9) Sienicki, K.; Winnik, M. A. *J. Chem. Phys.* **1987**, *87*, 2766.
(10) Stehfest, H. *Commun. ACM* **1970**, *13*, 47, 624.

Self-Diffusion of Hydrogenated Polybutadiene by Forward Recoil Spectroscopy

BUCKLEY CRIST*

Materials Science and Engineering, Northwestern University, Evanston, Illinois 60208

PETER F. GREEN,[†] RICHARD A. L. JONES, and EDWARD J. KRAMER

Materials Science and Engineering, Cornell University, Ithaca, New York 14856.

Received September 7, 1988; Revised Manuscript Received February 23, 1989

We report here a brief experimental study of interdiffusion of a crystallizable polymer in the molten state by forward recoil spectrometry (FRES). This technique has been used to great advantage for observing diffusion at temperatures above T_g in amorphous or noncrystallizable systems.[1-3] Certain limitations are found, however, due to specimen preparation in the case of crystalline polymers.

The materials used for this work are hydrogenated polybutadiene (HPB) and its deuterated analogue (DPB). A linear polymer of molecular weight $M_w = 424000$ g/mol, $M_w/M_n = 1.05$, and a three-arm star of total molecular weight $M_w = 75{,}400$ g/mol, $M_w/M_n = 1.10$, were employed. Fractional deuterium contents are $y = 0.40$ and $y = 0.44$ for linear DPB and star DPB, respectively. Synthesis and characterization of HPB and DPB are described elsewhere.[4,5] Important for this work is that the HPB/DPB pair in each case was prepared from the same parent polybutadiene, and hence each pair component has identical chain length and chemical microstructure. Both linear and star molecules contain $\sim$20 ethyl branches per 1000 C atoms which result from 1-2 (vinyl) additions of butadiene. These are thus model random copolymers of ethylene and butene-1, having a crystallinity of about 40% and a melting temperature of 105 °C.[6]

Specimens for FRES consisted of a relatively thick layer (ca. 5 μm) of HPB covered by a thin film (ca. 100 nm) of the analogous DPB. Thick HPB layers were solution cast on silicon wafers from hot (75 °C) cyclohexane solutions of 0.5–1.0% polymer concentration. It was found that directing an air flow over the solution minimized cracking as the film dried. The wafer was then heated to 125 °C for 5 min to complete the drying and to melt and recrystallize the HPB. The thin DPB films were formed by spinning solutions on a glass slide. Solvent, concentration, and temperature were the same as above. The DPB film was then floated off the glass in a distilled water bath and picked up on the HPB coated wafer. Completed bilayers were dried under ambient conditions for 1–2 h before the diffusion step.

Diffusion was initiated by heating the bilayer to 125 °C in a controlled-temperature air oven. Heating times were 180 s for the linear polymer and 1200 s for the three-arm star. Diffusion was terminated by an air quench. Interdiffusion time is this heating time minus 30 s, the interval required for the system to reach 125 °C.

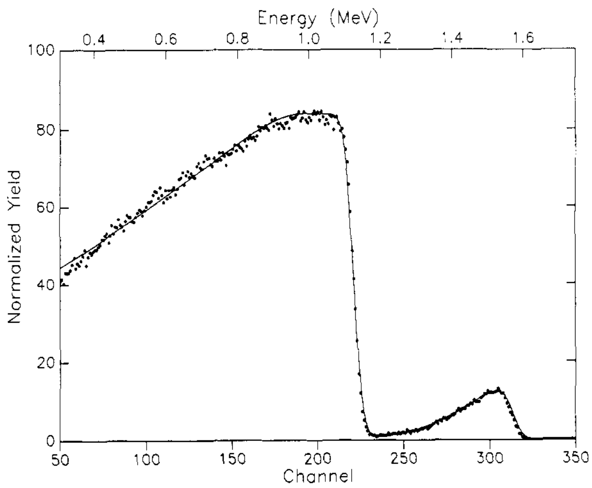

Figure 1. FRES data (●) and RUMP simulation (—) for three-arm star HPB/DPB interdiffused for 1170 s at 125 °C. Fitted parameters are $H = 110$ nm and $D = 2.4 \times 10^{-14}$ cm^2/s.

The concentration profile of DPB normal to the interface was determined by FRES with the apparatus described previously.[1] Experimental FRES data were fitted with the data analysis and simulation program "RUMP".[7] Concentration profiles are assumed to result from Fickian diffusion; thickness H of the undiffused DPB layer and the diffusion coefficient D are varied to produce the best fit of simulated to experimental data by a numerical optimization routine.[8] The scattering yields for H$^+$ and D$^+$ were calculated for atomic densities and cross-sections appropriate for HPB/DPB.

An example of an experimental FRES spectrum and the calculated FRES spectrum is shown in Figure 1 for the case of the three-arm star system that had interdiffused for 1170 s at 125 °C. Agreement is excellent, and the self-diffusion coefficient (interdiffusion of like chains mimics self-diffusion) is $D_s = 2.4 \times 10^{-14}$ cm^2/s, which is identical with the result obtained by small-angle neutron scattering (SANS) on the same HPB/DPB pair.[5] Similarly, $D_s = 1.1 \times 10^{-12}$ cm^2/s for the linear pair having $M_w = 424000$, very close to the value $D_s = 1.3 \times 10^{-14}$ cm^2/s obtained by extrapolating SANS results on linear HPB[4] to this molecular weight. It should be noted that fractional deuteration reduces the unfavorable thermodynamic interaction[9] between normal and labeled chains in the melt. For this linear DPB with $y = 0.40$ and a degree of polymerization $N = 7600$ (based on C$_4$H$_8$ repeats), the interaction term is calculated to be $\chi N = 1.3$, which will cause some "thermodynamic slowing down" at the earliest stages of interdiffusion. The modest difference between the present result with large linear chains and SANS studies on smaller chains is qualitatively consistent with enthalpic modification of the diffusion process, but the 20% effect is about the same size as the combined precision of the two techniques in question. It is not our purpose to pursue such effects here, beyond pointing out that the same experiment with a fully deuterated polymer ($y = 1$, $\chi \propto y^2$)[9] would have $\chi N = 8.7$, and the two components would have only limited miscibility.

Hence it is shown that FRES gives the same results as SANS for the interdiffusion of matched pairs of HPB and DPB. This enhances one's confidence in diffusion coefficients obtained by either method, but particularly the SANS technique. There it is *assumed* that concentration

---

[†] Present address: Sandia National Laboratories, Albuquerque, NM 87185.

0024-9297/89/2222-2857$01.50/0